Solid-state "magic-angle" sample-spinning nuclear magnetic resonance spectroscopic study of group III–V (13–15) semiconductors

Oc Hee Han, Hye Kyung C. Timken,[a] and Eric Oldfield
School of Chemical Sciences, University of Illinois at Urbana-Champaign, Urbana, Illinois 61801

(Received 28 June 1988; accepted 5 August 1988)

We have obtained ^{27}Al, ^{69}Ga, ^{71}Ga, ^{113}In, and ^{115}In static and "magic-angle" sample-spinning (MASS) solid-state nuclear magnetic resonance (NMR) spectra of a series of polycrystalline III–V semiconductors (AlN, AlP, AlAs, AlSb, GaN, GaP, GaAs, GaSb, InN, InP, InAs, and InSb) at magnetic field strengths of 8.45 and 11.7 T. Line-broadening mechanisms have been identified by comparing static and MASS NMR results. By applying the MASS technique, dipolar, first-order quadrupolar, and pseudodipolar interactions are removed. Thus, the MASS spectral linewidth (of the central, $1/2 \leftrightarrow -1/2$, transition) is dominated by exchange and/or second-order quadrupolar interactions. For compounds having the cubic zinc blende structure, the exchange interaction dominates, and exchange interaction constants can be determined. For AlP, AlAs, AlSb, GaP, GaAs, InP, and InAs, first-order quadrupole effects are evident as spinning sidebands (SSBs), due to the satellite transitions. These effects are due to a small distribution of electric field gradients caused by lattice defects, and result in an overall Lorentzian profile for the SSB envelope. For compounds having the hexagonal wurtzite structure (GaN and AlN), the second-order quadrupolar interaction is the main line-broadening mechanism, and we find isotropic chemical shifts δ_i of 333 ppm [from 1 M $Ga(NO_3)_3$] for GaN, and of 115 ppm [from 1M $Al(H_2O)_6Cl_3$] for AlN, and nuclear quadrupole coupling constant e^2qQ/h of 2.8 MHz for ^{69}GaN, 1.7 MHz for ^{71}GaN, and of 2.2 MHz for AlN.

INTRODUCTION

The extensive use of group III–V (IUPAC Groups 13, 15) semiconductors (e.g., GaAs, InP, InAs) in materials for electronics, information, and communications is due to the greater electron mobility and shorter excited state lifetimes in some III–V compounds, compared with those found in silicon semiconductors. These materials have thus made possible faster circuits and switches, permitting higher data processing rates. However, group III–V semiconductors have the disadvantage that they are more susceptible to structural defects. Nuclear magnetic resonance (NMR) is one of the few techniques which can, in principle, probe such defects down to the nearest-neighbor level.[1-8] In addition, NMR can give information about the nature of the chemical bonds and charge state of the atoms in a crystal. Group III–V semiconductor systems are particularly well suited for study by NMR, because most of the nuclei in these systems possess large magnetic moments, and are present in high natural abundance, unlike silicon semiconductors.

In this article, we present our preliminary results of ^{27}Al ($I = 5/2$, 100% abundance) ^{69}Ga ($I = 3/2$, abundance = 60.4%), ^{71}Ga ($I = 3/2$, abundance = 39.6%), ^{113}In ($I = 9/2$, abundance = 4.28%), and ^{115}In (I = 9/2, abundance = 95.72%) high-resolution solid-state "magic-angle" sample-spinning (MASS) NMR studies of polycrystalline, III–V semiconductors. Of the III–V semiconductors that we have examined (AlN, AlP, AlAs, AlSb, GaN, GaP, GaAs, GaSb, InN, InP, InAs, and InSb), all have Al, Ga, or In in tetrahedral coordination. Most have the cubic zinc blende structure,[9,10] which is expected to give a zero electric field gradient (efg) at the nucleus for perfect crystals,[11-13] while AlN, GaN, and InN have the hexagonal wurtzite structure,[9,10] and are expected to have modest efgs at the metal nucleus.

The broadening of the Al, Ga, and In NMR linewidths in the III–V semiconductors is expected to be primarily due to five interactions: dipolar,[1,2,14,15] pseudodipolar,[1,2,15] first- and second-order quadrupolar,[1-8] and exchange[1,14,16-18] interactions. To date, it has been a difficult task to identify the relative contributions from each of the different line-broadening mechanisms, most studies relying on second-moment calculations involving various theoretical models.[1-7,14-16] The MASS NMR technique[19] can, however, selectively remove some of these interactions, since rapid mechanical spinning of a sample at the magic angle (54.7°) with respect to the static field (H_0) averages all interactions described by second rank tensors. Thus, MASS removes broadenings due to dipolar, pseudodipolar, and first-order quadrupolar interactions. The only interactions remaining (for the central, $-1/2$, $1/2$, transition) in the MASS NMR spectra are thus the exchange and second-order quadrupolar interactions, together with any chemical shift dispersion due to "heterogeneity". The contribution of the second-order quadrupolar interaction can be independently assessed from field dependence measurements[20] (as can contributions from chemical shift dispersions) and for Ga and In, from the apparent chemical shifts of the two Ga and In isotopes at one magnetic field strength.[21]

The MASS NMR technique can also show, in principle,

[a] Present address: Mobil Research and Development Corporation, Paulsboro, NJ 08066-0480.

 0021-9606/88/226046-07$02.10

quadrupolar structure due to first order quadrupolar interactions,[11] since the satellite transitions break up into spinning sidebands (SSBs) which can be readily observed, due to their large peak signal-to-noise ratio. In III–V semiconductors, the satellite transitions giving rise to the SSBs are due to small distributions of efgs caused by point defects, and we show they are well described by a Lorentzian distribution, basically as described previously by Cohen.[22]

EXPERIMENTAL SECTION

Sample preparation

GaP, GaAs, GaSb, InN, InP, InAs, and InSb samples (99.9999%) were obtained from AESAR (Seabrook, NH) while AlN (99.8%), AlP (99.9%), AlAs (99.9%), and AlSb (99.999%) were obtained from CERAC (Milwaukee, WI). All materials were provided as lumps or polycrystalline pieces, which were ground by hand to coarse powders in order to obtain MASS NMR spectra.

Grey GaN (99.99%) was obtained from Atomergic Chemicals (Plainview, NJ) and yellow GaN (99.99%) was obtained from the Aldrich Chemical Company (Milwaukee, WI). These two samples were compared by powder x-ray diffraction, microchemical analysis, and NMR techniques. The powder patterns of both the GaN samples were in good agreement with published data.[23] However, the yellow GaN yielded a much broader x-ray powder diffraction pattern, and NMR linewidths indicated the more amorphous nature of this sample. Microchemical analysis also showed that the grey GaN had less impurities (experimental results, grey GaN, Ga = 80.8%, N = 16.03%, H = 0.01%: yellow GaN, Ga = 76.4%, N = 12.60%, H = 0.31%: theoretical values, Ga = 83.27%, N = 16.73%). We thus discarded preliminary results obtained on the yellow GaN sample, and further purified[24,25] the grey material by boiling in hot aqua regia for 48 h, in order to remove any unreacted gallium (which gives pure, colorless GaN, a grey coloration). The purified GaN was then filtered and washed with deionized water and methanol, then dried overnight at 100 °C. The resulting powder was very light grey.

X-ray powder diffraction patterns were obtained from grey GaN and yellow GaN with the use of a Norelco (Philips Electronics Instruments Inc., Mahwah, NJ) powder diffractometer, and atomic absorption analyses for both GaN samples were performed by either Galbraith Laboratories (Knoxville, TN) or the University of Illinois Microanalytical Laboratory.

Nuclear magnetic resonance spectroscopy

^{27}Al, ^{69}Ga, ^{71}Ga, ^{113}In, and ^{115}In static and MASS NMR spectra were obtained at 8.45 and 11.7 T using "home-built" spectrometers, which consist of Oxford Instruments (Osney Mead, Oxford, U.K.) 8.45 T 89 mm bore or 11.7 T 52 mm bore superconducting solenoid magnets, Nicolet Instrument Corporation (Madison, WI) model 1280 computers for data acquisition, and Amplifier Research (Souderton, PA) model 200L amplifiers for final rf pulse generation. Static spectra were obtained using home-built solenoidal probes, while MASS NMR spectra were obtained using a home-built probe equipped with a "Wind-mill"-type spinner.[21,26] Samples were spun in the range 6–8.5 kHz, with less than 20 Hz of fluctuation. Chemical shifts for Al and Ga are reported in ppm from external standards of 1 M $Al(H_2O)_6Cl_3$ or 1 M $Ga(NO_3)_3$ aqueous solutions, while In shifts are reported in ppm from external InP. More positive values correspond to low field, high frequency, paramagnetic or deshielded values (IUPAC δ scale). Line broadenings due to exponential multiplication were 10 to 100 Hz, depending on the linewidths.

RESULTS AND DISCUSSION

Cubic zinc blende structures

The following compounds studied have the cubic zinc blende structure: AlP, AlAs, AlSb, GaP, GaAs, GaSb, InP, InAs, and InSb. The measured NMR parameters for ^{27}Al, ^{69}Ga, ^{71}Ga, ^{113}In, and ^{115}In, the observed chemical shifts δ_{obs}, isotropic chemical shifts δ_i, and the full width at half-height (FWHH), are given in Table I, and representative NMR spectra are shown in Figs. 1, 2, and 3. The line-broadening interactions for the central transition of these compounds using MASS NMR are due, in principle, to exchange and/or second-order quadrupolar interactions, together with any chemical shift dispersion. However, no appreciable second-order quadrupolar interaction is in fact observed, as deduced from line shape and field dependence measurements, at 8.45 and 11.7 T. These results confirm that the exchange interaction overwhelmingly dominates the observed spectra, as convincingly demonstrated with, e.g., GaSb [Figs. 2(E) and 2(F)] and InSb [Figs. 3(G), 3(H), and 3(I)]. Also, our results exclude the possibility that the line broadening is due to a residual chemical shift dispersion.

Now, the spin exchange interaction between two nuclei is of the form $E_{jk} = A_{jk}\,\mathbf{I}_j \cdot \mathbf{I}_k$, where A_{jk} refers to the exchange coupling constant, and $\mathbf{I}_j$ and $\mathbf{I}_k$ are the nuclear spins.[14] The exchange interaction involves coupling between the nuclear spins via the nuclear spin–electron spin hyperfine interaction. It is therefore very sensitive to the electron energy states in both valence and conduction bands, and is particularly sensitive to energy surfaces far from the Fermi level, and so can in principle provide information about the band structure of these normally inaccessible regions. Van Vleck's equation states that the second moment for the exchange interaction is

$$h^2\langle \Delta\nu_j \rangle^2_{Av} = \tfrac{1}{3}\Sigma_f [\, (I_f(I_f+1)\Sigma_k A^2_{jk}(r_{jk})\,], \qquad (1)$$

where the subscripts f refer to different nuclear species.[16] According to Anderson's theory, A_{jk} is given by[1]

$$A_{jk} = \left(\frac{8}{9\pi}\right)\gamma_e^2\gamma_j\gamma_k\hbar^2\Omega^2\zeta_j\zeta_k\Psi_j^2(0)\Psi_k^2(0)m^*r_{jk}^{-4}, \qquad (2)$$

where Ω is the atomic volume, γ_e, γ_j, and γ_k are the gyromagnetic ratios of the electron, nucleus j, and nucleus k, respectively, r_{jk} is the distance between nuclei j and k, and

$$\zeta_j = \frac{[\,\Psi_j(0)^*_{\text{hole}}\Psi_j(0)_{\text{electron}}\,]_{\text{solid}}}{[\,\Psi_j^2(0)\,]_{\text{atom}}}, \qquad (3)$$

where $\Psi_j^2(0)$ is the probability of finding an outer (s) electron of atom j at the nucleus, and

TABLE I. Solid-state Al, Ga, and In NMR chemical shifts and linewidths for III–V seminconductors.

Aluminum NMR					
				δ_i[d]	
Compound	Static[a] FWHH (kHz)	MASS[b] FWHH (kHZ)	δ_{obs}[c] (ppm)	This work	Ref.33
AlN	6.63	1.15	114	115 ± 1	98 ± 3
AlP	4.84	0.34	142	142 ± 1	139 ± 2
AlAs	4.22	0.22	130	130 ± 1	110 ± 2
AlSb	4.13	0.66	70	70 ± 1	66 ± 2

Gallium NMR										
	^{69}Ga			^{71}Ga			δ_i[d]			
Compound	Static[a] FWHH (kHz)	MASS[b] FWHH (kHz)	δ_{obs}[c] (ppm)	Static[a] FWHH (kHz)	MASS[b] FWHH (kHz)	δ_{obs}[c] (ppm)	This work	Ref. 32	Ref. 33 (theory)	Ref. 38[e]
GaN	8.72	2.69	320	5.67	1.15	330	333 ± 2	...	...	...
GaP	2.65	0.17	307	3.62	0.25	307	307 ± 1	300	292	334
GaAs	2.55	1.17	216	3.31	1.55	216	216 ± 1	200	192	194
GaSb	7.09	5.8	-47 ± 2	8.76	7.4	-46 ± 2	-46 ± 2	-80	39	-46

Indium NMR								
	^{113}In			^{115}In			δ_i[d]	
Compound	Static[a] FWHH (kHz)	MASS[b] FWHH kHz)	σ_{obs}[c] (ppm)	Static[a] FWHH (kHz)	MASS[b] FWHH (kHz)	δ_{obs}[c] (ppm)	This work	Ref. 32
InP	4.65	2.42	0	3.38	0.74	0	0	0
InAs	7.04	4.56	-178	4.26	3.22	-178	-178	-200
InSb	15.4	14.7	-777 ± 4	13.0	13.3	-776 ± 4	-777 ± 4	-850

[a]Full width at half-height, in kHz, for static spectra.
[b]Full width at half-height, in kHz, for the central transition of MASS spectra.
[c]Observed chemical shift. Except for GaN and AlN, the observed chemical shift is the same as the isotropic chemical shift (see the text). Errors are ± 1 ppm unless otherwise noted.
[d]Isotropic chemical shift, in ppm.
[e]Chemical shift for GaSb was set to -46 for purposes of comparison.

$$m^* = 4\frac{(m_e^*)^{3/2}(m_h^*)^{3/2}}{(m_e^* + m_h^*)^2}, \tag{4}$$

where m_e^* and m_h^* are the electron and hole effective masses, respectively. The exchange interaction has no angular dependence, so unlike the dipolar, pseudodipolar, and quadrupole interactions, it does not average out on MASS. It is important to note here that the exchange interaction calculated here only results in line broadening when the interaction is between *unlike* nuclear spins, and the line shape from this interaction is known to be Gaussian.[17,18] We find that the line shapes of the central peaks of the MASS NMR spectra are indeed Gaussian, having a FWHH of[27]

$$\begin{aligned}\text{FWHH} &= 2(2\ln 2)^{1/2}\langle \Delta\nu_j^2\rangle_{\text{Av}}^{1/2} \\ &= 2.35\langle \Delta\nu_j^2\rangle_{\text{Av}}^{1/2}. \end{aligned} \tag{5}$$

From the FWHH of the MASS NMR spectra shown in Figs. 1–3, and using the above equations, we can determine the nuclear spin exchange coupling constants A_{jk}.

Table II shows A_{jk} values, or the relationship between them, obtained when only the four nearest neighbor nuclei are considered. From these A_{jk} values, energy band information is available, in principle. Unfortunately, limiting the accuracy of the calculation is the integration over momentum space in both the valence and conduction bands, and further theoretical work is needed in order to obtain useful energy band information from the A_{jk} values. Table III shows cw NMR second moment data from other groups after subtraction of the dipolar interaction, which have been used to obtain the exchange coupling constants. Also, the Table shows the second moments of our central peaks in the MASS NMR experiment. We believe our results indicate that MASS can give more accurate exchange coupling constant values when there are several comparable line-broadening interactions, as in, for example, GaAs, since MASS excludes the first-order quadrupolar line broadening which, unlike dipolar line broadening, cannot be subtracted theoretically from the observed peak widths.

The lack of any appreciable second-order quadrupolar interaction indicates that the quadrupolar interaction is small. However, in the MASS NMR spectra of a few samples, the increased signal-to-noise ratios obtained over those seen with the static spectra make it possible to observe the effects of first-order quadrupolar interactions, which are

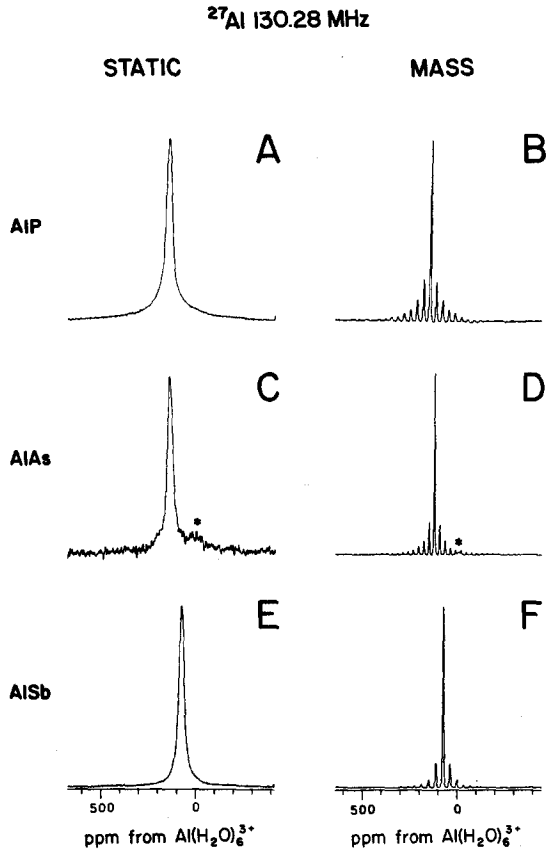

FIG. 1. 11.7 T ^{27}Al static and MASS NMR spectra of a series of III–V compounds. (A) AlP, static, 5500 scans, 1 s recycle time. (B) AlP, MASS at 8.7 kHz, 300 scans, 40 s recycle time. (C) AlAs, static, 1500 scans, 40 s recycle time. (D) AlAs, MASS at 8.3 kHz, 5400 scans, 1 s recycle time. (E) AlSb, static, 2000 scans, 12 s recycle time. (F) AlSb, MASS at 4.8 kHz, 300 scans, 60 s recycle time. Asterisks indicate a possible Al_2O_3 impurity.

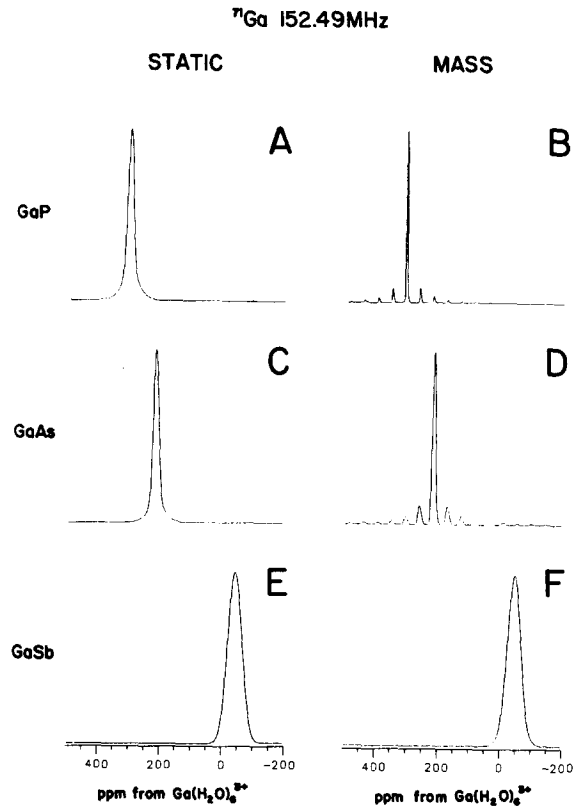

FIG. 2. 11.7 T ^{71}Ga static and MASS NMR spectra of a series of III–V compounds. (A) GaP, static, 1200 scans. (B) GaP, MASS at 6.7 kHz, 1600 scans. (C) GaAs, static, 820 scans. (D) GaAs, MASS at 6.7 kHz, 2000 scans. (E) GaSb, static, 1300 scans. (F) GaSb, MASS at 6.0 kHz, 2800 scans. Typical recycle times were from 300 ms to 1 s.

manifested as SSBs from the satellite ($m \leftrightarrow m-1$, $m \neq 1/2$) transitions. The overall SSB patterns reveal a distribution of efgs associated with defects, since well-defined powder pattern edges are absent,[28–30] as can be seen for example in Figs. 4(A) and 4(B). Since the first-order quadrupolar interaction affects only the satellite transitions, plotting the intensities of the SSBs maps out the efg distribution. Typical results are shown in Fig. 4. Figure 4(C) shows the observed data points for ^{69}Ga of GaP (circles) and a least-squares fit to the data. Good agreement is obtained using a Lorentzian line shape with a FWHH of 16.0 $\pm$ 0.2 kHz. The FWHH of such distributions for AlP, AlAs, AlSb, GaP, GaAs, and InP, for each isotope, are given in Table IV. Our results are in good agreement with Cohen's theory,[22] which assumes randomly distributed point charge defects, and a linear sum of the electric field gradients produced by each defect. According to Cohen's theory, the shape of the component arising from transitions, $m \leftrightarrow m-1$ ($m \neq 1/2$) in an imperfect crystal would be Lorentzian, with a FWHH, Γ_m, of

$$\Gamma_m = |2m-1| \frac{4\pi^2}{3\sqrt{3}} \frac{N\beta e^2 Q}{I(2I-1)h}, \tag{6}$$

where N is the number of point defects per unit volume, β is a multiplication factor, e is the electron charge, and Q is the electric quadrupole moment. $\overline{\Gamma}_m$ can be obtained by replacing the $|2m-1|$ in Γ_m by that which is weighted according to each component's relative transition probability, $|\overline{2m-1}|$, for all m except $m = 1/2$. $\overline{\Gamma}_m$ reflects the FWHH of the Lorentzian function of the sum of all the satellite transitions. MASS separates the satellite transitions from the central transition completely, even in the presence of the efg distribution, in such samples.

The FWHH for each semiconductor should be linearly proportional to the value of N for each compound. However, only the product value $N\beta$ can be obtained from our MASS NMR experiments, and further work with systematically doped samples, with known N values, is required, in order to independently assess β.

It is, nevertheless, possible to use the chemical shift data to determine the nature of the chemical bonds in such materials, and to estimate semiempirically the parameters of the energy structure, as outlined previously by Ilin and Masterovs.[31] Table I shows Al, Ga, and In NMR chemical shifts for the III–V semiconductors we have studied, along with previously published results, for comparison. Other groups[32–34] have obtained a good correlation between chemical shifts and the Szigetti effective charge (e_s^*). However, we find for Ga that the best correlation between chemical shift and effective charge is obtained by using the localized effective

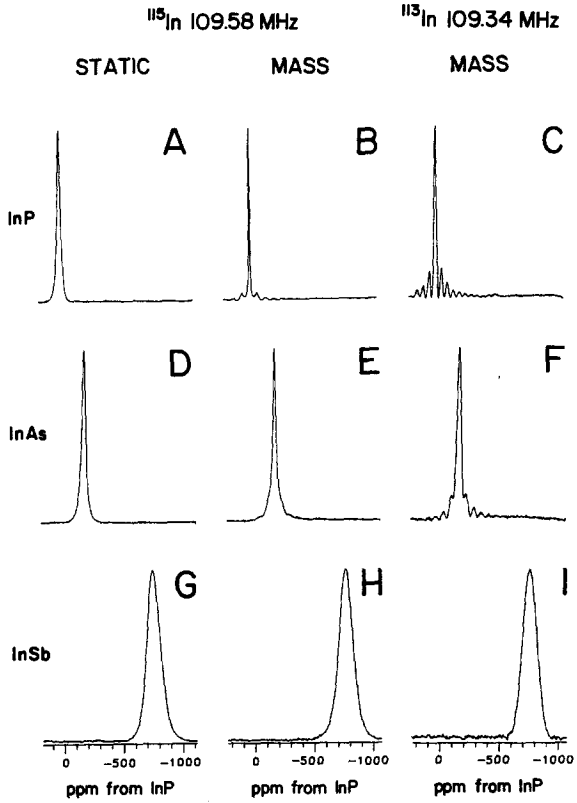

FIG. 3. 11.7 T ^{115}In static, MASS, and ^{113}In MASS NMR spectra of a series of III–V compounds. (A) ^{115}In NMR of InP, static, 4500 scans. (B) ^{115}In NMR of InP, MASS at 6.4 kHz, 6000 scans. (C) ^{113}In NMR of InP, MASS at 15 300 scans. (D) ^{115}In NMR of InAs, static, 4600 scans. (E) ^{115}In NMR of InAs, MASS at 6.4 kHz, 6700 scans. (F) ^{113}In NMR of InAs, MASS at 7.0 kHz, 10 500 scans. (G) ^{115}In NMR of InSb, static, 4200 scans. (H) ^{115}In NMR of InSb, MASS at 6.4 kHz, 5000 scans. (I) ^{113}In NMR of InSb, MASS at 6.4 kHz, 13 300 scans. Typical recycle times were 500 ms and 1 s.

charge (e_l^*)[35] rather than e_s^*.[35] Both e_l^* and e_s^* describe the microscopic effective charge, which is the localized charge at specific positions in the crystal. Our results imply that the effective charge state of Ga in Ga semiconductors is better described by e_l^* than by e_s^*. For In compounds, the best correlation is obtained by using the transverse effective charge[35] e_T^*, rather than e_l^*. Table V and Fig. 5 show the data and the correlations. e_T^*, which is the macroscopic effective charge (and is model independent), includes contributions from charges localized near the ion sites, as well as charges distributed throughout the unit cell. It is not surprising, therefore, that the In compounds have the best correlation with e_T^*, while the Ga compounds have the best correlation with e_l^*, since In nuclei in In semiconductors (with a smaller band

TABLE II. Exchange coupling constant A_{jk} calculated using the full width at half-height of the central transition.

Compound	Nucleus	A_{jk}[a] (10^{-34} kJ)
AlP	^{27}Al	$A_{^{27}Al^{31}P} = 0.96 \pm 0.04$
AlAs	^{27}Al	$A_{^{27}Al^{75}As} = 0.28 \pm 0.04$
AlSb[b]	^{27}Al	$6.68A^2_{^{27}Al^{121}Sb} + 8.98A^2_{^{27}Al^{123}Sb} = 3.5 \pm 0.1$
GaP	^{69}Ga	$A_{^{69}Ga^{31}P} = 0.5 \pm 0.1$
	^{71}Ga	$A_{^{71}Ga^{31}P} = 0.70 \pm 0.06$
GaAs	^{69}Ga	$A_{^{69}Ga^{75}As} = 1.47 \pm 0.05$
	^{71}Ga	$A_{^{71}Ga^{75}As} = 1.95 \pm 0.03$
GaSb[b]	^{69}Ga	$6.68A^2_{^{69}Ga^{121}Sb} + 8.98A^2_{^{69}Ga^{123}Sb} = 270 \pm 50$
	^{71}Ga	$6.68A^2_{^{71}Ga^{121}Sb} + 8.98A^2_{^{71}GA^{123}Sb} = 430 \pm 30$
InP	^{113}In	$A_{^{113}In^{31}P} = 6.8 \pm 0.3$
InSb[b]	^{113}In	$6.68A^2_{^{113}In^{121}Sb} + 8.98A^2_{^{113}In^{123}Sb} = 1700 \pm 160$
	^{115}In	$6.68A^2_{^{115}In^{121}Sb} + 8.98A^2_{^{115}In^{123}Sb} = 1410 \pm 60$

[a] Only the four nearest neighbor nuclei are considered.
[b] The unit is 10^{-68} kJ^2 rather than 10^{-34} kJ.

TABLE III. The second moment of the central transition.

Compound	Nucleus	Second moment (kHz^2) This work	Ref. 16[b]
AlP	^{27}Al	0.021 ± 0.002	···
AlAs	^{27}Al	0.009 ± 0.002	···
AlSb	^{27}Al	0.079 ± 0.003	···
GaP	^{69}Ga	0.005 ± 0.003	···
	^{71}Ga	0.011 ± 0.002	···
GaAs	^{69}Ga	0.25 ± 0.02	0.72 ± 0.03
	^{71}Ga	0.43 ± 0.02	1.1 ± 0.1
GaSb	^{69}Ga	6 ± 1	5.6 ± 0.4
	^{71}Ga	9.9 ± 0.7	8.5 ± 0.7
InP	^{113}In	1.1 ± 0.4	···
InSb	^{113}In	39 ± 4	···
	^{115}In	32 ± 3	19 ± 1

[a] Equation (6) was used to calculate the second moment $\langle \Delta\nu_j^2 \rangle_{Av}$ from the FWHH of the central peak in the MASS NMR spectrum.
[b] Second moment calculated from the relationship $\delta H_{pp}^2 = 4\Delta H^2$ for a Gaussian line shape in the derivative spectrum. The second moment due to dipolar interaction was subtracted from ΔH^2.

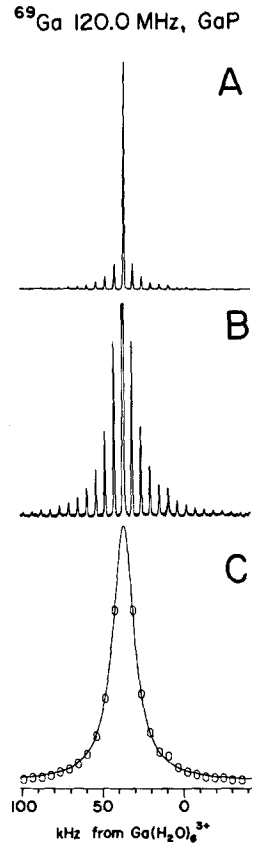

FIG. 4. 11.7 T ^{69}Ga MASS NMR spectra of GaP. (A) MASS at 5.6 kHz, 6900 scans, 300 ms recycle time. (B) Expansion of (A). (C) Least-squares fit of satellite transition in (A) with a Lorentzian function. The central peak is excluded. The circles represent data points and the solid line is the least-squares fit.

TABLE IV. Full width at half-height of satellite transition distribution for first-order quadrupolar interaction in III–V semiconductors.

Compound	Nucleus	FWHH[a] (kHz)
GaP	^{69}Ga	16.0 ± 0.2
	^{71}Ga	13.0 ± 0.2
GaAs	^{69}Ga	21.0 ± 0.3
	^{71}Ga	18.0 ± 0.2
AlP	^{27}Al	12.9 ± 0.1
AlAs	^{27}Al	8.1 ± 0.1
AlSb	^{27}Al	6.1 ± 0.4
InP	^{113}In	11.3 ± 0.3

[a]Full width at half-height, in kHz.

gap energy) have more delocalized electron interactions than Ga nuclei have in Ga semiconductors. In addition, the bigger polarizability of the In nucleus may play a role. It is to be expected that the best correlation for the chemical shifts of the Al compounds would be with e_l^* rather than with e_T^*, as with Ga compounds, but there is at present a lack of e_l^* data to confirm this prediction.

Wurtzite structures

AlN, GaN, and InN possess hexagonal wurtzite structures, and have two different atomic distances for the four nearest neighbors, as well as two different distances for the 12 next-nearest neighbors.[9,10,33] Therefore, nonzero electric field gradients are expected. We show in Fig. 6(A) the ^{71}Ga static NMR spectrum of grey GaN. It consists of two resonances, a broad component at 450 ppm, and a narrower component at 330 ppm. The broad feature is thought to be an impurity, since its intensity decreases after purification in aqua regia, Fig. 6(B). In addition, the intensity of the broad component decreases in the following sequence, yellow GaN ≫ grey GaN > purified grey GaN, as does the hydrogen content of the sample. Thus, we believe that the 330 ppm feature is characteristic of pure GaN.

Since ^{69}Ga has a larger quadrupole moment and lower Larmor frequency than ^{71}Ga,[36] resolved second-order structure is apparent in both static and MASS NMR spectra, Figs. 6(D) and 6(E). From these results, e^2qQ/h and δ_i information can be obtained via line shape simulation,[37] Fig.

TABLE V. Effective charges and dielectric constants for the zinc blende structure semiconductors.

Compound	e_T^* [a]	ϵ_∞ [a]	e_s^* [b]	e_l^* [a]
AlP	2.28	7.6	0.71	···
AlAs	2.30	9.0	0.63	···
AlSb	1.93	10.2	0.47	···
GaP	2.04	8.5	0.58	0.96
GaAs	2.16	10.9	0.50	0.78
GaSb	2.15	14.4	0.39	0.41
InP	2.55	9.6	0.66	1.36
InAs	2.53	12.3	0.53	1.01
InSb	2.43	15.6	0.41	0.53

[a]From Ref. 35.
[b]$e_s^* = 3e_T^*/(\epsilon_\infty + 2)$ are calculated from given e_T^* and ϵ_∞ values (Ref. 35).

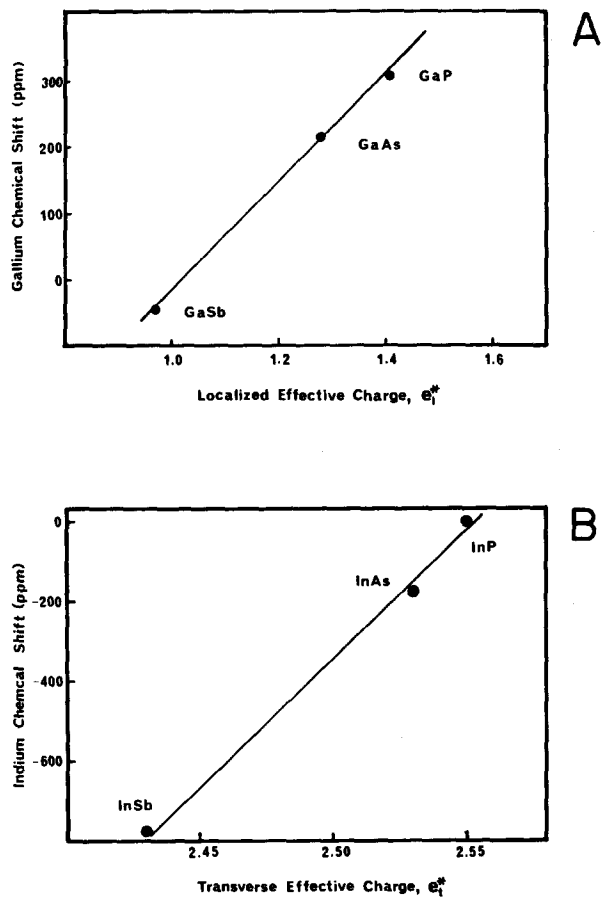

FIG. 5. (A) Plot of Ga isotropic chemical shift δ_i vs the localized effective charge e_l^*. (B) Plot of In isotropic chemical shift δ_i vs the transverse effective charge e_T^*.

6(F). We find $\delta_i = 333$ ppm, and $e^2qQ/h = 2.75$ MHz for ^{69}Ga (and $e^2qQ/h = 1.73$ MHz for ^{71}Ga) with $\eta \sim 0.25$. For ^{27}Al in AlN, the second-order quadrupolar shift can be used to obtain δ_i and e^2qQ/h information. For a spin 5/2 system, for

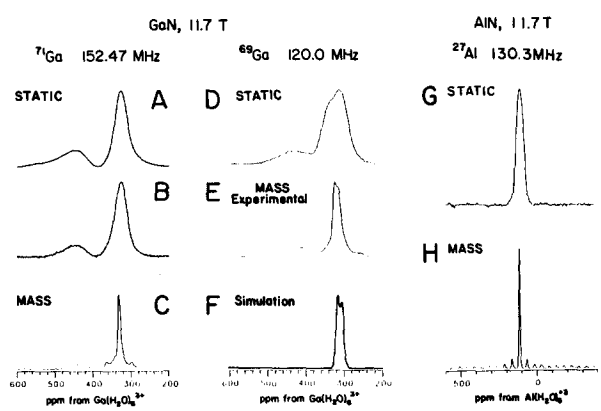

FIG. 6. 11.7 T static and MASS NMR spectra of GaN and AlN. (A) ^{71}Ga static, unpurified sample from Atomergic, 800 scans. (B) ^{71}Ga static, purified in aqua regia for 2 days, 1350 scans. The poorer signal-to-noise ratio is due to a smaller sample size. Other spectra were obtained from a purified sample. (C) ^{71}Ga MASS at 5.2 kHz, 320 scans. (D) ^{69}Ga static, 3700 scans. (E) ^{69}Ga MASS at 6.0 kHz, 1840 scans. (F) Simulation of (E), having $e^2qQ/h = 2.75$ MHz and $\eta = 0.25$. Typical recycle times were 10 s. (G) ^{27}Al NMR of AlN, static, 1200 scans, 40 s recycle time. (H) ^{27}Al NMR of AlN, MASS at 6.3 kHz, 300 scans, 60 s recycle time.

a powder sample, and for the central transition only, the second-order quadrupolar shift from the isotropic chemical shift δ_i is given by[21]

$$\sigma_{QS}(1/2) = -\frac{3\times 10^4}{5}\left(\frac{e^2qQ}{h\nu_0}\right)^2\left(1+\frac{\eta^2}{3}\right) \text{ (ppm)}. \quad (8)$$

For AlN, the apparent chemical shifts are 113.6 ppm (at 11.7 T) and 112.0 ppm (at 8.45 T) which yield $e^2qQ/h \approx 2.2$ MHz and $\delta_i = 115$ ppm (assuming $\eta = 0$). No In NMR of InN was obtained, presumably because of an excessively large e^2qQ/h value.

The preliminary results presented above show that MASS NMR techniques can separate NMR line-broadening mechanisms in III–V semiconductors, which were difficult using other NMR techniques. MASS NMR averages all interactions described by second rank tensors, removing linebroadening due to dipolar, pseudodipolar, and first-order quadrupolar interactions. Thus, only exchange and second-order quadrupolar interaction contribute to the MASS NMR linewidths of the central transitions. Field dependence measurements of the linewidth, and of the chemical shift, show that the exchange interaction is the dominant line-broadening mechanism for zinc blende structure, while second-order quadrupolar effects dominate the linewidths of the wurtzite materials.

ACKNOWLEDGMENTS

We thank Dr. Hee Cheon Lee for helpful discussion. This work was supported in part by the United States National Science Foundation Solid-State Chemistry Program (Grant No. DMR 86-15206).

[1]R. K. Sundfors, Phys. Rev. **185**, 458 (1969).
[2]R. K. Hester, A. Sher, J. F. Soest, and G. Weisz, Phys. Rev. B **10**, 4262 (1974).
[3]E. H. Rhoderick, J. Phys. Chem. Solids **8**, 498 (1958).
[4]M. K. Cueman, R. K. Hester, A. Sher, J. F. Soest, and I. J. Lowe, Phys. Rev. B **12**, 3610 (1975).
[5]D. G. Andrianov, V. V. Karataev, M. G. Mil'vidskii, and Yu. B. Muravlev, Sov. Phys. Semicond. **17**, 57 (1983).
[6]D. J. Oliver, J. Phys. Chem. Solids **11**, 257 (1959).
[7]E. H. Rhoderick, Philos. Mag. **3**, 545 (1958).
[8]W. E. Carlos and S. G. Bishop, Appl. Phys. Lett. **49**, 528 (1986).
[9]H. Walker and H. Weiss, *Solid State Physics*, edited by F. Seitz and D. Turnbull (Academic, New York, 1956), Vol. 3, p. 1.
[10]*Structure Reports*, edited by A. J. C. Wilson (Oosthoeck, Utrecht, 1913–1928), Vol. 1, pp. 76–79.
[11]A. Abragam, *Principles of Nuclear Magnetism* (Oxford University, New York, 1961), Chap. 7.
[12]O. Kanert and M. Mehring, *NMR Basic Principles and Progress*, edited by P. Diehl, E. Fluck, and R. Kosfeld (Springer, New York, 1971), Vol. 3, p. 1.
[13]I. Solomon, Phys. Rev. **110**, 61 (1958).
[14]R. G. Shulman, J. M. Mays, and D. W. McCall, Phys. Rev. **100**, 692 (1955).
[15]M. Engelsberg and R. E. Norberg, Phys. Rev. B **5**, 3395 (1972).
[16]R. G. Shulman, B. J. Wyluda, and H. J. Hrostowski, Phys. Rev. **109**, 808 (1958).
[17]M. A. Ruderman and C. Kittel, Phys. Rev. **96**, 99 (1954).
[18]J. H. Van Vleck, Phys. Rev. **74**, 1168 (1948).
[19]E. R. Andrew, *Progress in Nuclear Magnetic Resonance Spectroscopy*, edited by J. W. Emsley *et al.* (Pergamon, New York, 1971).
[20]A. Samoson, Chem. Phys. Lett. **119**, 29 (1985).
[21]H. K. C. Timken and E. Oldfield, J. Am. Chem. Soc. **109**, 7669 (1987).
[22]M. H. Cohen, Philos. Mag. **3**, 564 (1958).
[23]R. Juza and H. Hahn, Z. Anorg. Allg. Chem. **239**, 282 (1938).
[24]W. C. Johnson, J. B. Parsons, and M. C. Crew, J. Phys. Chem. **36**, 2651, (1932).
[25]R. B. Zetterstrom, J. Mater. Sci. **5**, 1102 (1970).
[26]R. A. Wind, F. E. Anthonio, M. J. Duijvestijn, J. Smidt, J. Trommel, and G. M. C. de Vette, J. Magn. Reson. **52**, 424 (1983).
[27]Reference 11, p. 107.
[28]S. G. Greenbaum, D. J. Treacy, B. V. Shanabrook, J. Comas, and S. G. Bishop, J. Non-Cryst. Solids **66**, 133 (1984).
[29]S. G. Greenbaum, D. J. Treacy, J. Comas, S. G. Bishop, and B. V. Shanabrook, in *Proceedings of the 17th International Conference on the Physics of Semiconductors*, edited by J. D. Chadi and W. A. Harrison (Springer, New York, 1985), p. 821.
[30]S. G. Greenbaum, R. A. Marino, K. J. Adamic, and C. Case, J. Non-Cryst. Solids **77&78**, 1285 (1985).
[31]N. P. Il'in and V. F. Masterov, Sov. Phys. Solid State **20**, 321 (1978).
[32]H. Lütgemeier, Z. Naturforsch. Teil A **19**, 1297 (1964).
[33]R. E. J. Sears, Phys. Rev. B **22**, 1135 (1980).
[34]R. E. J. Sears, Phys. Rev. B **18**, 3054 (1978).
[35]G. Lucovsky, R. M. Martin, and E. Burstein, Phys. Rev. B **4**, 1367 (1971).
[36]From Bruker NMR Table and CRC Handbook of Chemistry and Physics.
[37]S. Ganapathy, S. Schramm, and E. Oldfield, J. Chem. Phys. **77**, 4360 (1982).
[38]D. C. Look, Phys. Status Solidi B **50**, K97 (1972).